AD-A096 563 TEXAS UNIV AT AUSTIN APPLIED RESEARCH LABS F/6 17/1
INVESTIGATION OF A PARAMETRIC ACOUSTIC RECEIVING ARRAY FOR MOBI--ETC(U)
NOV 80 C R CLUBERTSON, R A LAMB, D F ROHDE N00024-77-C-6200
UNCLASSIFIED ARL-TR-80-53 NL

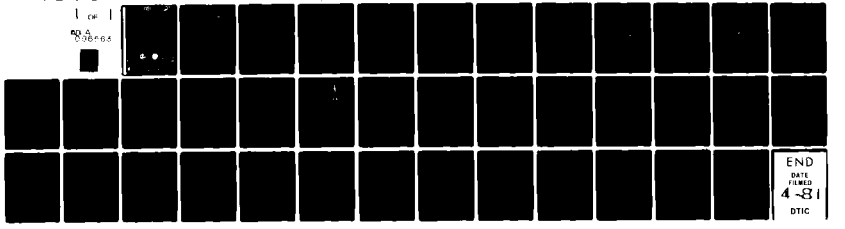

END
DATE FILMED
4-81
DTIC

ARL-TR-80-53

Copy No. 34

INVESTIGATION OF A PARAMETRIC ACOUSTIC RECEIVING ARRAY FOR MOBILE APPLICATIONS

Quarterly Progress Report No. 4 and
Final Report under Contract N00024-77-C-6200, Item 0011

C. Robert Culbertson
Robert A. Lamb
David F. Rohde

APPLIED RESEARCH LABORATORIES
THE UNIVERSITY OF TEXAS AT AUSTIN
POST OFFICE BOX 8029, AUSTIN, TEXAS 78712

5 November 1980

Final Report

3 August 1979 - 2 August 1980

APPROVED FOR PUBLIC RELEASE;
DISTRIBUTION UNLIMITED.

Prepared for:

NAVAL SEA SYSTEMS COMMAND
DEPARTMENT OF THE NAVY
WASHINGTON, DC 20362

UNCLASSIFIED

SECURITY CLASSIFICATION OF THIS PAGE *(When Data Entered)*

REPORT DOCUMENTATION PAGE	READ INSTRUCTIONS BEFORE COMPLETING FORM
1. REPORT NUMBER	2. GOVT ACCESSION NO. AD-A096563	3. RECIPIENT'S CATALOG NUMBER (9)
4. TITLE (and Subtitle) (6) INVESTIGATION OF A PARAMETRIC ACOUSTIC RECEIVING ARRAY FOR MOBILE APPLICATIONS.	5. TYPE OF REPORT & PERIOD COVERED OPR & Final Technical Report. 3 Aug [redacted]79— 2 Aug [redacted]80
	6. PERFORMING ORG. REPORT NUMBER (14) ARL-TR-80-53
7. AUTHOR(s) (10) C. Robert Culbertson, Robert A. Lamb, David F. Rohde	8. CONTRACT OR GRANT NUMBER(s) (15) N00024-77-C-6200
9. PERFORMING ORGANIZATION NAME AND ADDRESS Applied Research Laboratories, The University of Texas at Austin, Austin, Texas 78712	10. PROGRAM ELEMENT, PROJECT, TASK AREA & WORK UNIT NUMBERS Item 0011 (12) 40
11. CONTROLLING OFFICE NAME AND ADDRESS (11) Naval Sea Systems Command, Department of the Navy, Washington, DC 20362	12. REPORT DATE 5 Nov [redacted]80
	13. NUMBER OF PAGES 36
14. MONITORING AGENCY NAME & ADDRESS *(if different from Controlling Office)*	15. SECURITY CLASS. *(of this report)* UNCLASSIFIED
	15a. DECLASSIFICATION DOWNGRADING SCHEDULE

16. DISTRIBUTION STATEMENT *(of this Report)*

Approved for Public Release; Distribution Unlimited.

17. DISTRIBUTION STATEMENT *(of the abstract entered in Block 20, if different from Report)*

18. SUPPLEMENTARY NOTES

19. KEY WORDS *(Continue on reverse side if necessary and identify by block number)*

PARRAY
Nonlinear acoustics
Parametric reception
Vibration
Turbulence
Phase-locked loop receiver

20. ABSTRACT *(Continue on reverse side if necessary and identify by block number)*

The parametric acoustic receiving array (PARRAY) exploits the nonlinearity of acoustic waves in water to achieve directional reception of low frequency acoustic waves using only two high frequency transducers and associated electronics. In mobile applications the parametric receiver will be required to operate under the influence of sensor motion, and in water that is sometimes turbulent. This report describes these two areas of technical risk which are pertinent to the successful implementation of PARRAYs on submarine platforms. Analysis, fabrication, and testing of a phase-locked loop receiver is described.

DD FORM 1 JAN 73 1473 EDITION OF 1 NOV 65 IS OBSOLETE

UNCLASSIFIED 404434

SECURITY CLASSIFICATION OF THIS PAGE *(When Data Entered)*

20. (Cont'd)

This type of receiver is shown to be well suited for demodulating the output of a mobile PARRAY hydrophone and reducing the detrimental effects of transducer motion on the PARRAY. For mobile applications the transducers will be moving with respect to the water and will create some degree of turbulence near the sensors. Investigations of the effects of turbulence on the operation of the PARRAY are discussed. These investigations allow predictions of the magnitude of amplitude and phase fluctuations generated at the PARRAY hydrophone output for known levels of turbulence.

TABLE OF CONTENTS

LIST OF FIGURES

I. INTRODUCTION

The PARRAY utilizes the nonlinearity of acoustic wave propagation in water to synthesize a virtual array between two transducers, the pump and hydrophone. This virtual array has the directivity characteristics of a conventional end-fire array of the same length as the pump-hydrophone separation, but with a considerable reduction in the number of transducers required. The main advantage of using a PARRAY in a submarine application, therefore, is that a narrow, conical receiving beam can be obtained with minimum hardware in the water. This receiving beam has a front-to-back ratio and a vertical directivity which discriminate against surface noise at the mid frequencies. Also, since the virtual array is synthesized in the water, it is reformed (or stabilized) at the speed of sound during maneuvers and changes in heading. Because there are no transducer elements between pump and hydrophone, the PARRAY may be less sensitive to flow noise as boat speed increases. These characteristics of the parametric receiving array contribute to its attractiveness in submarine passive sonar applications. However, there are possible performance limitations of a mobile PARRAY that need to be considered. In particular, the effects of transducer vibration and of turbulence in the PARRAY interaction volume may constrain the usefulness of the PARRAY in a mobile application and therefore should be studied.

Previous work[1-3] on the PARRAY was conducted using band elimination crystal filters to suppress the high level pump signal and permit recovery of the information in the sidebands. However, for most mobile applications there are potential problems using this technique. There will almost surely be some vibration of the transducers, which can smear narrowband signals and degrade the performance of the PARRAY. A phase-locked loop (PLL) receiver has been shown in this study to be well suited to the solution of this problem. The receiver must be capable

of processing signals with very wide dynamic range with minimum noise and distortion; this requires the system to have good linearity and very low noise throughout. The development of a PLL receiver suitable for mobile PARRAY applications is discussed in Section II of this report.

Because the parametric receiver effectively forms an array in the medium between pump and hydrophone, its operation is sensitive to the state of the medium in this region. The presence of air bubbles, pieces of hardware, or significant temperature or flow velocity gradients will modify the synthesized array and alter its performance. In particular, at moderate or high boat speeds, the turbulence produced in the wake of the pump transducer may have several effects on the performance of the parametric receiver. The turbulence will act as a volume distributed, low frequency acoustic source that will increase the noise level of the parametric receiver. Turbulence will also scatter the acoustic waves propagating between pump and hydrophone, thereby producing random amplitude and phase fluctuations in the detected acoustic signals. These effects of turbulence are investigated in Section III.

A summary of the results of this study is contained in Section IV.

II. PARRAY PHASE-LOCKED LOOP (PLL) RECEIVER DEVELOPMENT

The parametric acoustic receiving array (PARRAY) utilizes the nonlinearity of the medium to synthesize a directional acoustic sensor. For this reason the PARRAY exhibits a response to transducer vibration that is significantly different from a linear array.[4] Figure 1 depicts the PARRAY, which uses the nonlinear interaction of an injected high frequency pump wave and low frequency acoustic signal waves in the medium to generate modulation sidebands about the pump frequency that are detected by the receiver electronics. Relative longitudinal motion of the PARRAY transducers phase modulates the carrier and sideband signals received by the PARRAY hydrophone and can degrade PARRAY performance.

The phase-locked loop receiver of the type developed in this study is well suited for demodulating PARRAY hydrophone signals and reducing the effect of transducer vibration on the PARRAY output. The purpose of the study described in this section was to design, fabricate, and evaluate a PLL (or mixer) receiver for mobile PARRAY applications.

A. Project Accomplishments

1. Phase-Locked Loop Analysis

Relative longitudinal motion of the PARRAY transducers phase modulates the signals received by the PARRAY hydrophone. Relative displacement on the order of the pump wavelength generates intermodulation between the acoustically generated signals and the vibration signals. It has been shown[4] that the PARRAY hydrophone output in the presence of transducer vibration is a carrier signal phase modulated by the sum of an acoustic signal and the vibration signal.

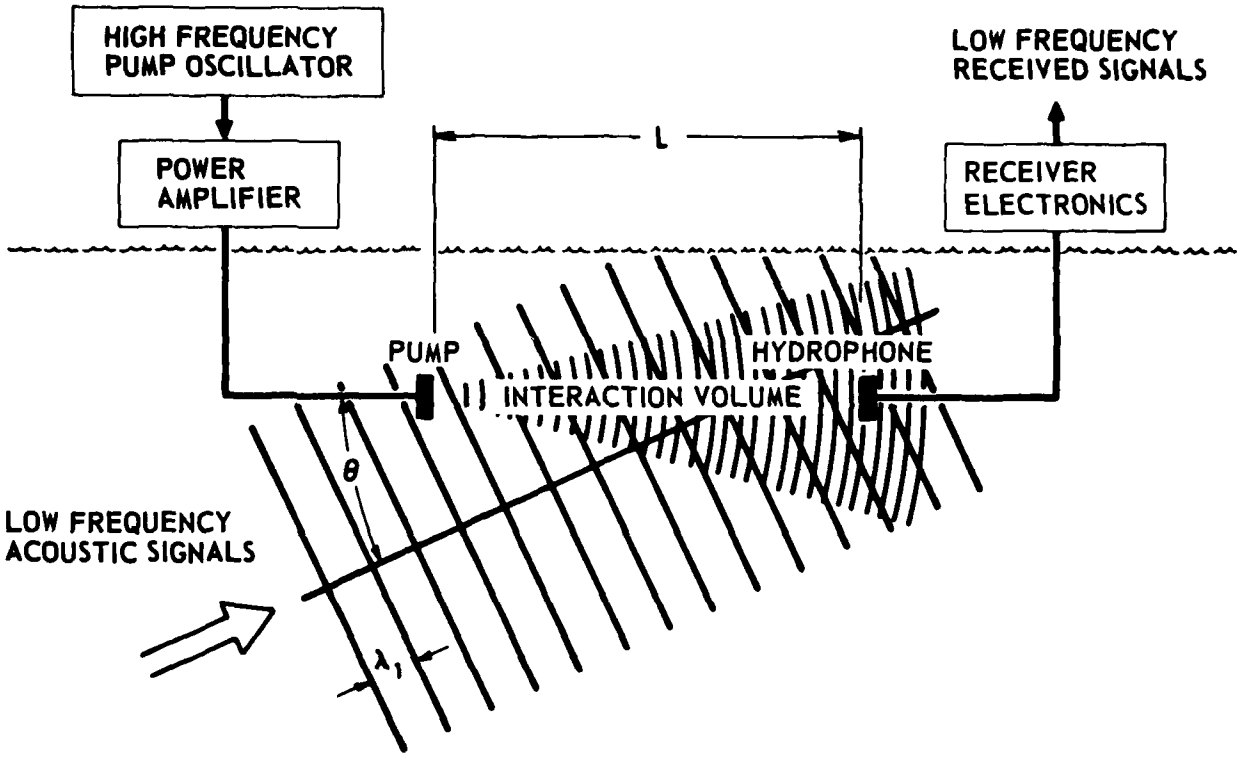

FIGURE 1
PARRAY FUNCTIONAL DIAGRAM

ARL:UT
AS-77-1398-P
CRR - GA
12 - 8 - 77
Vers. A

The spectrum of this type of signal is shown in Fig. 2. This figure shows how the intermodulation products generated by transducer vibration tend to mask the desired acoustically generated sideband signals, which makes detection of narrowband sideband signals difficult. A PLL demodulator can reduce the level of the intermodulation signals relative to the acoustic signals by linearly demodulating the phase modulated signal present at the PARRAY hydrophone output.

Analysis of the PLL receiver, which assumes all components are linear,[5] predicts no intermodulation between the acoustic and vibration signals at the PLL output. For PARRAY applications with high level transducer vibration, nonlinearities in loop components make this analysis inadequate. Nonlinearities in PLL components produce harmonics as well as intermodulation products. The level of the intermodulation products is important in mobile PARRAY applications because the PARRAY demodulator must process low level acoustic signals in the presence of high level vibration generated signals.

A number of authors[6,7,8] have studied the effects of nonlinearity in PLL demodulators. These studies are not applicable to the PARRAY PLL operation because of assumptions that are not valid for the type PLL needed for PARRAY applications. For this reason analysis has been performed to allow prediction of the PLL output when the PLL input is the expected PARRAY hydrophone output. This analysis uses a perturbation series technique to separately determine the effects of phase detector and voltage controlled oscillator nonlinearities on the PLL output.[9] This analysis showed that for the particular circuit used in this study the voltage controlled oscillator (VCO) generated most of the intermodulation present at the PLL output. Using the measured value of VCO nonlinearity the predicted levels of intermodulation signals were compared with experimental measurements.

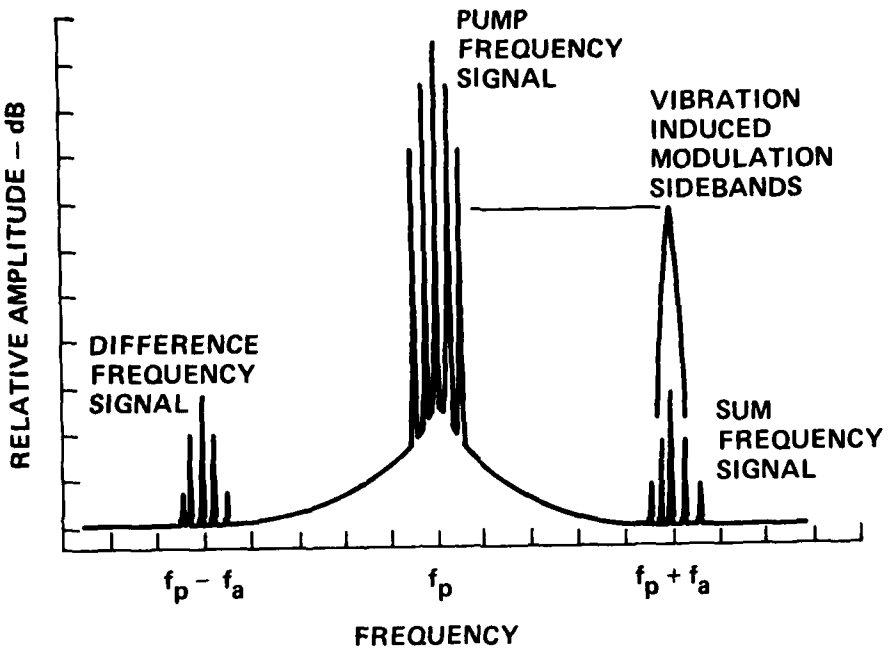

FIGURE 2
PARRAY SPECTRUM WITH VIBRATING TRANSDUCERS

$$s(t) = A_p \sin (\omega_p t + A_a \sin \omega_a t + A_v \sin \omega_v t)$$

ACOUSTICAL SIGNAL

VIBRATIONAL SIGNAL

ARL:UT
AS-80-1678
RAL - GA
10 - 9 - 80

2. Prototype Receiver Design and Fabrication

A block diagram of the prototype PLL receiver is shown in Fig. 3. This receiver is designed for 65 kHz carrier frequency but can be modified for use at other frequencies by changing the VCO. This receiver has both a high and low input impedance port and variable loop filter frequency, which allow flexibility of operation. Additional circuit details and a schematic can be found in Ref. 9. Results of a number of performance tests of this receiver will be described in the next two sections of this report.

3. Electronic Measurements of PLL Performance

Both electronic and acoustic tests were made in order to measure the characteristics of the PLL receiver. Electronic measurements were used to determine PLL characteristics using a wide range of well controlled input characteristics. Acoustic tests were less well controlled because of physical limitations; however, they allowed verification of PLL performance under realistic conditions.

Four basic types of electronic measurements were performed tc determine the characteristics of the PLL receiver. These measurements were frequency response, receiver noise, intermodulation distortion, and VCO electronic tuning response. These measurements are described in Ref. 9; however, a summary of their results is given here. The PLL frequency response verified basic PLL operation as predicted by linear PLL theory. The results of these tests were in very good agreement with theoretical predictions.

Receiver noise tests measured the electronic noise of the PLL receiver under operating conditions in order to measure the minimum sideband level that can be detected by the receiver. These measurements showed that the PLL receiver could detect sidebands with sideband-to-carrier ratios (SBCR) of approximately -160 to -163 dB. Receiver noise limitations may be a problem in some applications. Present notch filter

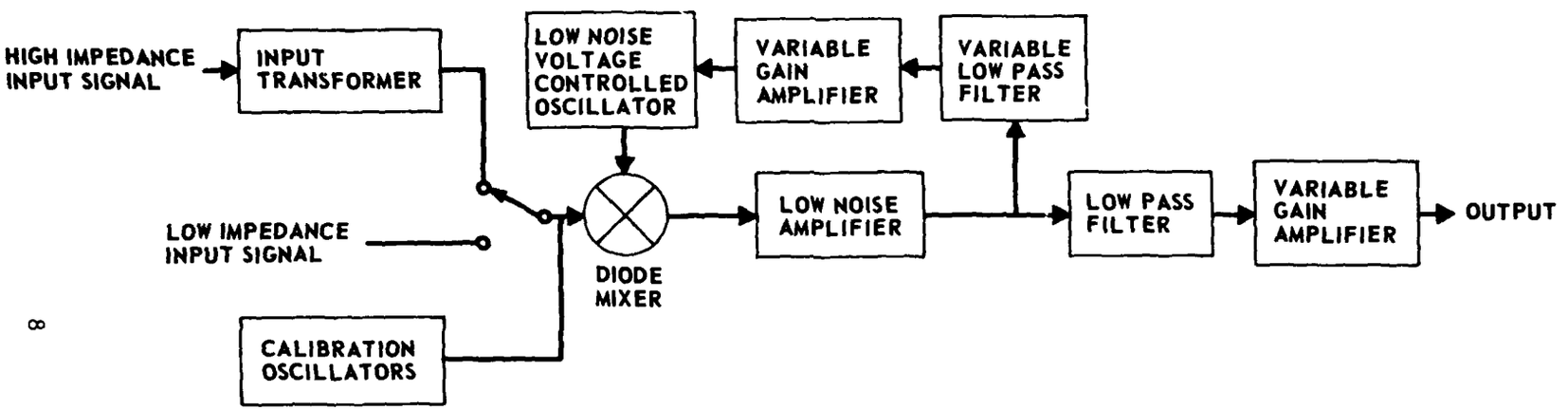

FIGURE 3
EXPERIMENTAL MIXER-RECEIVER BLOCK DIAGRAM

ARL-UT
AS-80-773
RAL-GA
2-7-80

receivers are capable of detecting signals with SBCR's on the order of -170 dB.

Intermodulation distortion measurements used simulated PARRAY signals to measure the level of intermodulation present at the PLL output. The results of these measurements were in good agreement with acoustic data and theoretical predictions.

Measurements of VCO electronic tuning response allowed prediction of intermodulation levels as well as maximum vibration levels over which the PLL can be expected to operate. A plot of these maximum vibration levels is shown in Fig. 4. This curve shows the maximum transducer displacement amplitude as a function of vibration frequency that can be tracked by the VCO used in the present study. Displacement amplitudes in excess of this maximum will result in greatly increased intermodulation distortion levels.

4. Acoustic Measurements

Acoustic measurements were performed to evaluate the PLL receiver as a part of the PARRAY system with a vibrating transducer. The results of these tests demonstrated the effectiveness of a PLL in reducing the effects of transducer vibration on the PARRAY output.

Figure 5 depicts the system used to demonstrate the effect of transducer vibration on the PARRAY using two types of demodulators. The system consists of a PARRAY pump and hydrophone, a low frequency sound source, and associated electronics. A motor driven system allows variation of both the frequency and amplitude of the PARRAY hydrophone displacement. This displacement was measured using a low frequency accelerometer. The PARRAY hydrophone output was fed simultaneously into a notch filter and PLL receiver to allow measurement of the PLL receiver reduction of intermodulation sideband amplitudes.

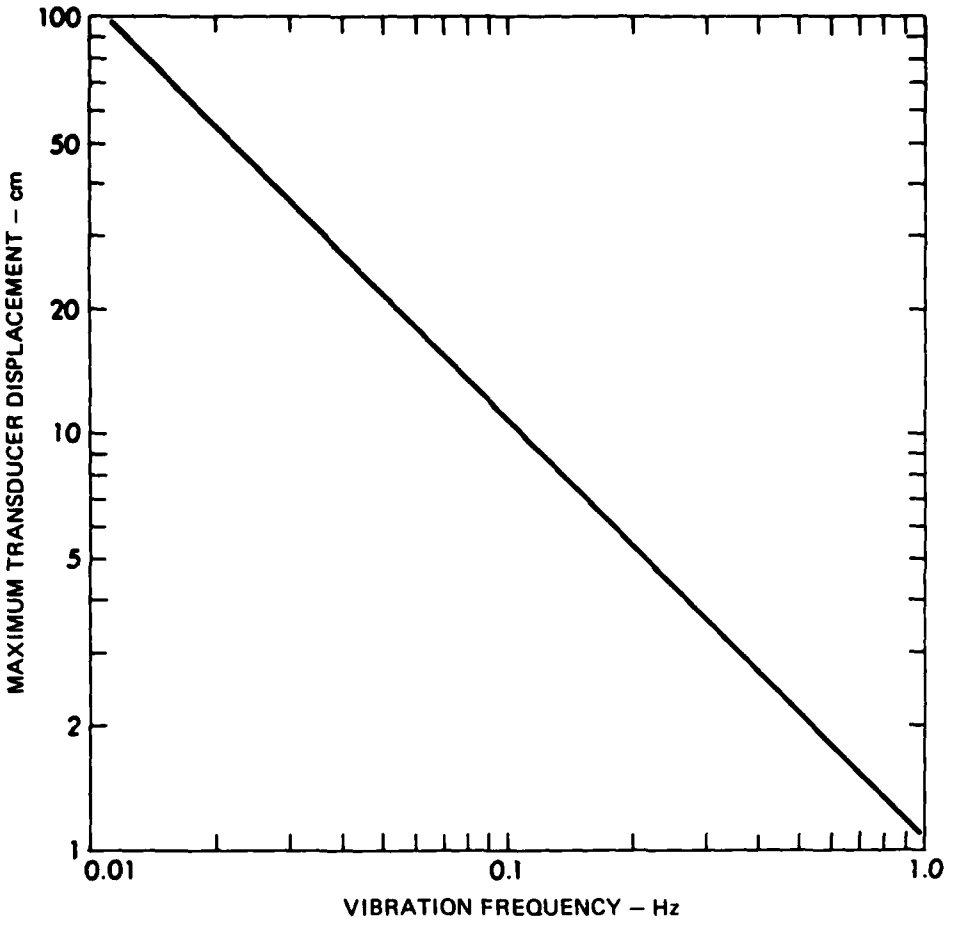

FIGURE 4
MAXIMUM TRANSDUCER DISPLACEMENT AS A FUNCTION OF FREQUENCY FOR PRESENT PLL RECEIVER OPERATION

ARL:UT
AS-80-1770
RAL - GA
11-7-80

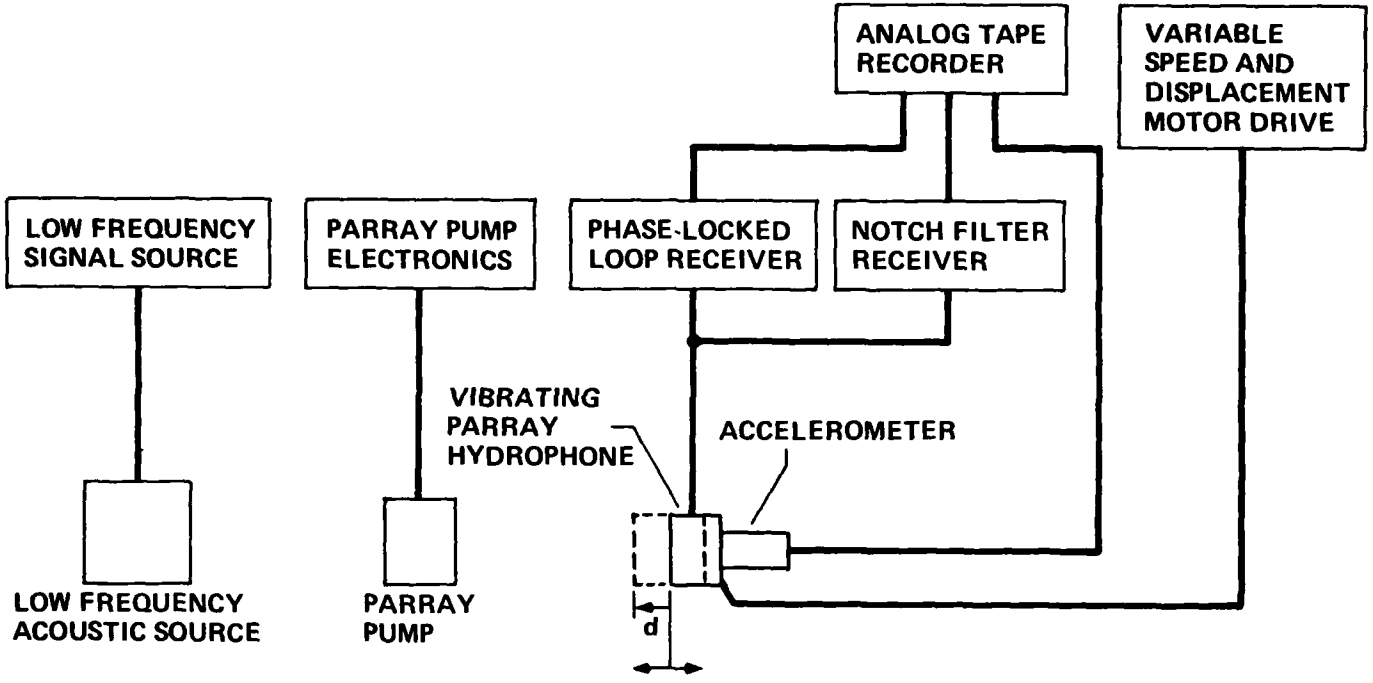

FIGURE 5
BLOCK DIAGRAM OF PLL VIBRATION EXPERIMENT

ARL:UT
AS-80-1680
RAL - GA
10 - 9 - 80

Figure 6 compares the output spectrums of the two receivers while the PARRAY was receiving a 151 Hz acoustic tone. The upper curve shows the output spectrum of the notch filter receiver and the lower curve the output spectrum of the PLL receiver. The spectral broadening of the 151 Hz tone is caused by vibration of the hydrophone at a 0.3 Hz rate with a peak displacement of approximately 6 mm. These curves demonstrate a reduction of the vibration induced intermodulation sidebands of approximately 50 dB (relative to the 151 Hz tone) by the PLL receiver.

Twelve data sets similar to the curves in the previous figure are summarized in Figs. 7 and 8. These curves show the amplitude of the intermodulation sidebands relative to the acoustic signal level as a function of vibration frequency. Figure 7 shows the level of these sidebands for a peak transducer displacement of 6 mm. Figure 8 shows similar data for a transducer displacement of 2 and 4 mm. Theoretical curves on these figures show the predicted sideband amplitude using the transducer displacement measured by the accelerometer. These curves demonstrate a 20-40 dB reduction of the amplitude of intermodulation sidebands and are within 6 dB of theoretical predictions.

B. Summary and Conclusions

The purpose of the study described in this section was to design, fabricate, and evaluate a PLL receiver for mobile PARRAY applications. The goals of this study have been met by analyzing PLL operation with the PARRAY, developing a prototype receiver, and evaluating the receiver using an experimental PARRAY system. Analysis and experiments have shown the value of the narrowband PLL demodulator in PARRAY applications. Very good performance has been demonstrated by the prototype PLL in reducing the effects of transducer vibration on the PARRAY.

The PLL demodulator has been shown to be a very good receiver for use in mobile PARRAY applications where transducer vibration on the order of the pump wavelength is expected. More research is recommended in the areas of higher frequency receiver design and lower noise electronics for use in future PARRAY applications.

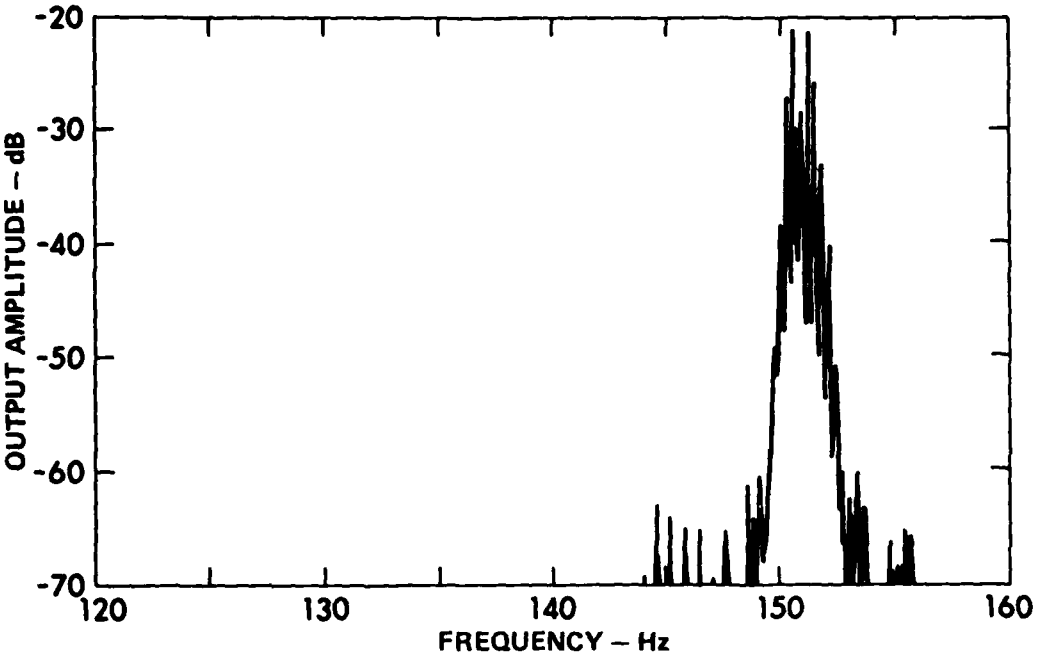

(a) BER-4 OUTPUT WITH VIBRATING HYDROPHONE

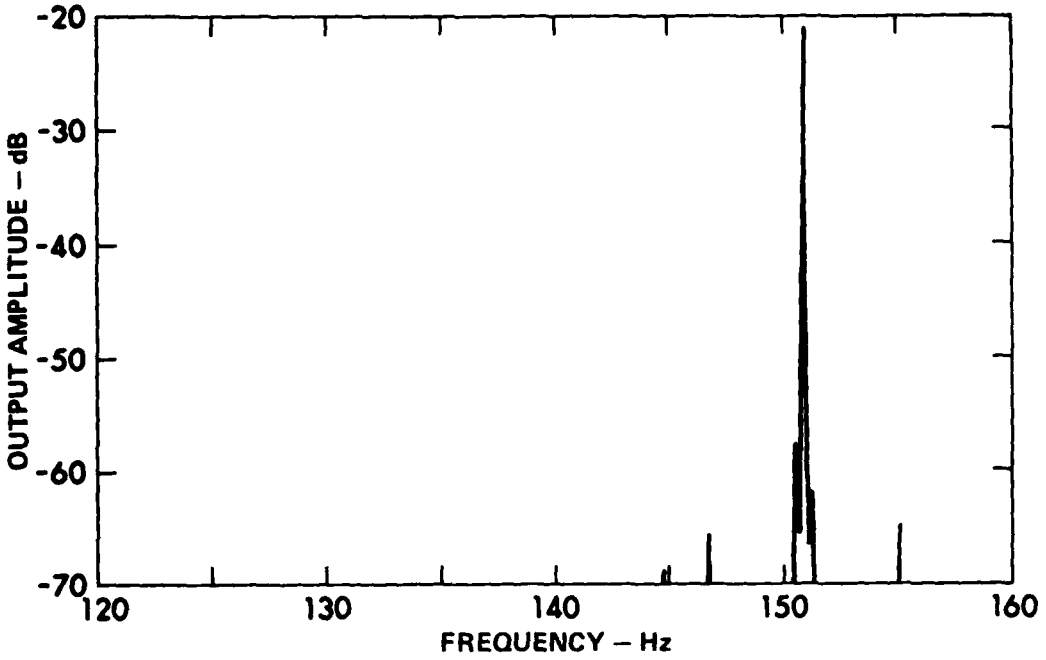

(b) PHASE-LOCKED LOOP RECEIVER OUTPUT
WITH VIBRATING HYDROPHONE

FIGURE 6

COMPARISON OF DATA FROM PARRAY RECEIVERS FOR VIBRATING HYDROPHONE

($d = 5.8$ mm $\quad f_v = 0.3$ Hz)

ARL:UT
AS-80-1611-P
RAL - GA
9 - 5 - 80

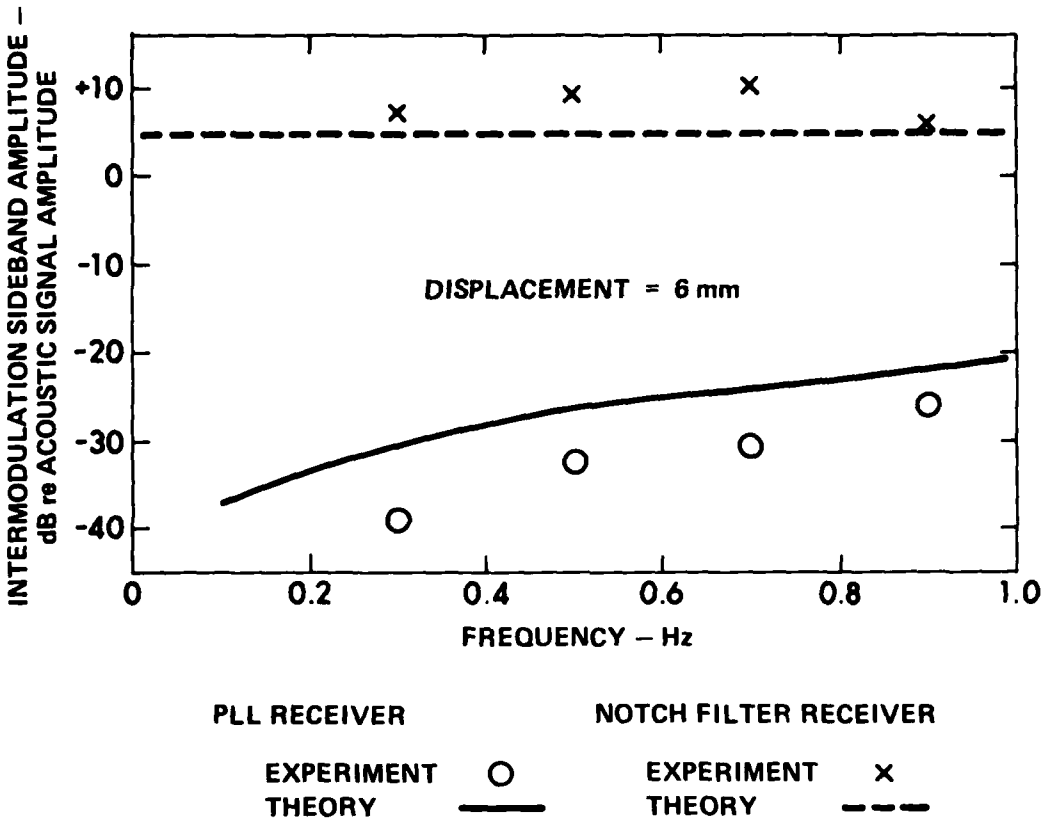

FIGURE 7

VIBRATIONAL SIDEBAND DATA FOR 6 mm DISPLACEMENT

ARL:UT
AS-80-1773-S
RAL - GA
11-4-80

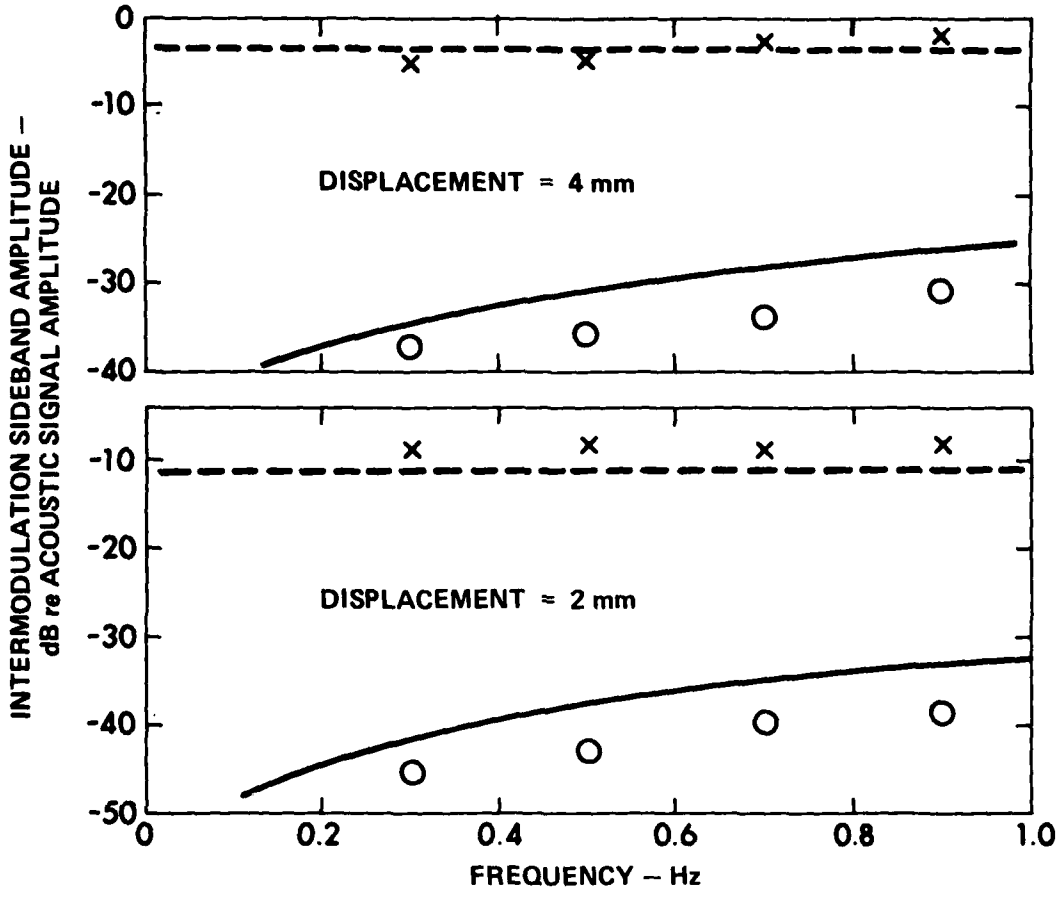

FIGURE 8

VIBRATIONAL SIDEBAND DATA FOR 2 mm AND 4 mm DISPLACEMENT

ARL:UT
AS-80-1774-S
RAL - GA
11-4-80

III. INVESTIGATION OF THE EFFECTS OF TURBULENCE ON PARRAY OPERATION

A. Theoretical Results

Suppose a parametric receiver consisting of pump transducer and hydrophone is placed on a vessel moving from right to left through the medium. If the transducers are placed clear of the boundary layer turbulence produced by the vessel's hull, then the situation can be modeled by considering two stationary transducers in a fluid that flows from left to right, as shown in Fig. 9. The flow will separate in the region of the pump transducer, and vortices will form. At some distance downstream from the transducer, the vortices will decompose into the random velocity field that characterizes turbulence. The dimensions and intensity of the turbulence are dependent upon the flow velocity and upon the geometry of the rigid boundaries associated with the flow.

It can be shown[10] that the eddies associated with turbulent flow may be treated as "patches" of variable refractive index. These patches, or inhomogeneities, will scatter the acoustic waves propagating in the interaction region between pump transducer and hydrophone. As a result of scattering, amplitude and phase fluctuations in both pump and sideband waves will occur.

The fluctuations in the sideband waves are a source of noise to the parametric receiver that can act to degrade its performance in the detection of acoustic signals. The purpose of the theoretical work discussed in this section is to obtain expressions for the amplitude and fluctuations in the sideband waves in terms of parameters of the turbulence.

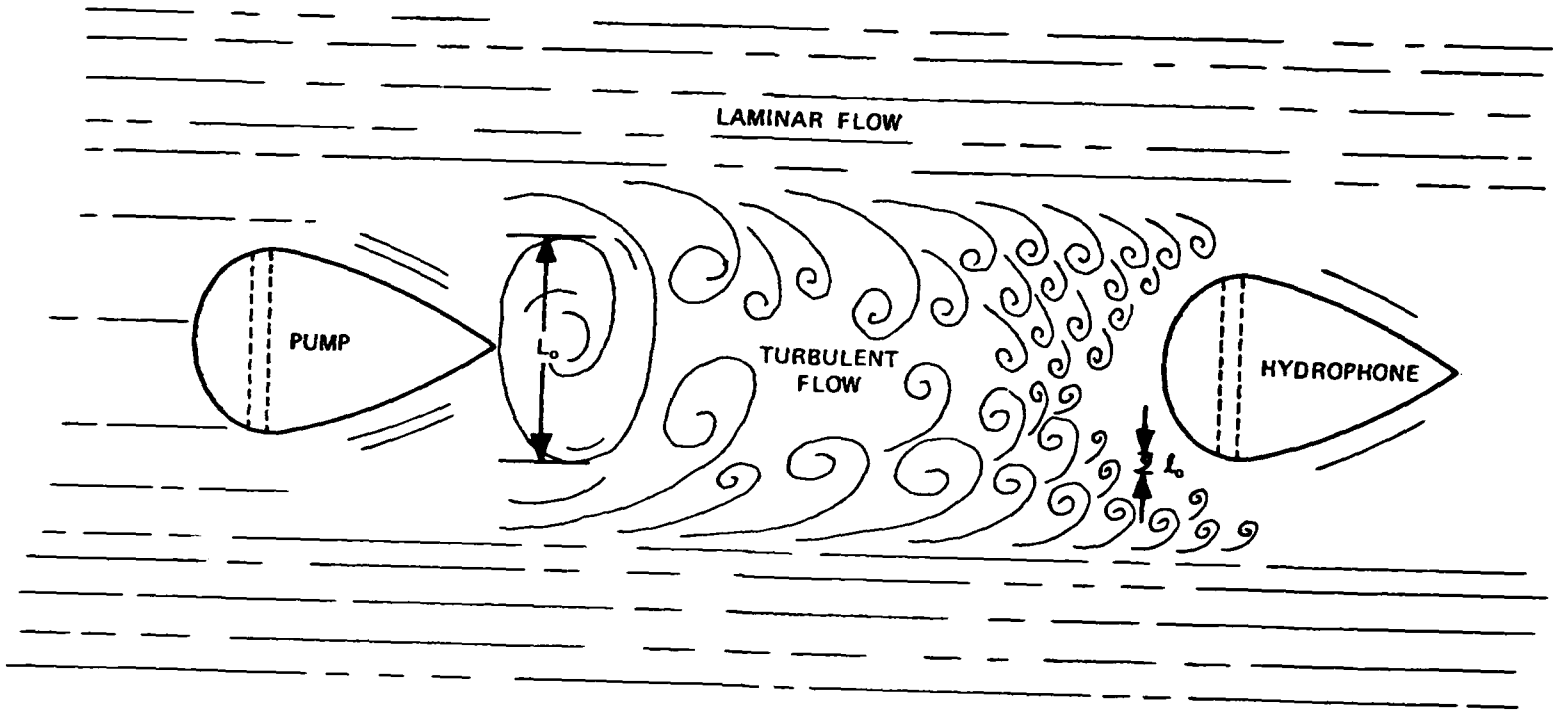

FIGURE 9
GENERATION OF TURBULENCE IN INTERACTION REGION

ARL:UT
AS-79-1278
CRC - GA
8-27-79

1. Analysis for Weak Turbulence

A detailed analysis of the effects of weak turbulence on the performance of a mobile parametric receiver is given in Ref. 10. In this analysis, the acoustic waves are modeled as follows. The pump wave is assumed to be spherically spreading, but confined to a narrow beam by the directivity of the pump transducer. There are fluctuations, B_p and S_p, in the amplitude and phase, respectively, of the pump wave. For the "small perturbation" analysis in Ref. 10, these fluctuations are assumed to be small (i.e., less than 10% of the mean amplitude or phase). The signal wave is assumed to be planar and, because of its relatively low frequency, is assumed to have a negligible level fluctuation due to the turbulence in the interaction region.

The interaction of these two first order waves (the pump and signal waves) produces an array of virtual sources in the region between pump and hydrophone.

The second order pressure radiated from each virtual source will have amplitude and phase fluctuations, $B_{\pm}$ and $S_{\pm}$, respectively, due to scattering caused by turbulence. The second order pressure $p_{\pm}$ detected by the hydrophone of the parametric receiver will therefore depend upon the fluctuation terms B_p, S_p, $B_{\pm}$, and $S_{\pm}$.

The mean squared amplitude and phase fluctuations in the pressure $p_{\pm}$ may be shown to be

$$\langle B_{PR}^2 \rangle \doteq 0.1415\, C_n^2\, k_p^{7/6} L^{11/6} \quad , \tag{1}$$

and

$$\langle S_{PR}^2 \rangle \doteq 0.8889\, \sqrt{\langle \mu^2 \rangle}\, k_p^2\, aL \quad , \tag{2}$$

where

C_n is the turbulence structure constant,
k_p is the acoustic wave number at frequency ω_p,
L is the pump-hydrophone separation,
$\langle\mu^2\rangle$ is the mean squared refractive index variation, and
a is the mean correlation distance of the refractive index.

Equations (1) and (2) are expressions for fluctuations in the detected pressure $p_{\pm}$ in terms of the acoustic wave number, the array length L, and the turbulence parameters, C_n, $\langle\mu^2\rangle$, and a. These results indicate that the fluctuations increase with the intensity of the turbulence in the interaction region. This is because the amplitude and phase fluctuations increase with C_n^2 and $\langle\mu^2\rangle$, respectively, and both of these parameters are related to turbulence intensity. Also from Eqs. (1) and (2) it can be seen that the fluctuations increase with the separation L of the pump and hydrophone. This is reasonable, because as L increases, the number of scatterers that lie in the paths of the propagating waves is increased.

The results in Eqs. (1) and (2) are based on the assumption that the fluctuations in the pump and interaction frequency waves remain small. This amounts to assuming that the turbulence is sufficiently weak for given array lengths and acoustic wave numbers that small perturbation theory is applicable to the problem. For stronger turbulence, where the methods of small perturbation theory no longer apply, it is useful to make a simpler theoretical model.

2. Analysis for Strong Turbulence

It is shown in Ref. 10 that the fluctuations in the sideband pressure $p_{\pm}$ are approximately equal to corresponding fluctuations in the pump wave. In other words,

$$\langle B_{PR}^2\rangle \doteq \langle B_p^2\rangle \quad ,$$

and

$$\langle S_{PR}^2 \rangle \doteq \langle S_p^2 \rangle \quad .$$

As an approximate solution to the problem of strong turbulence, "smooth perturbation theory" for linear waves may be used to obtain the following results.

$$\langle B_{PR}^2 \rangle \doteq 0.13\, C_n^2\, k_p^{7/6} L^{11/6} \quad , \tag{3}$$

and

$$\langle S_{PR}^2 \rangle \doteq 0.50 \sqrt{\pi}\ \langle u^2 \rangle\, k_p^2\, aL \quad . \tag{4}$$

It can be seen that these results are approximately equal to the expressions in Eqs. (1) and (2), the difference being in the numerical constants. This difference is more severe for the phase fluctuations than for the amplitude fluctuations. However, Eqs. (3) and (4) are valid for rms fluctuation levels up to about 50%, whereas Eqs. (1) and (2) are valid only up to rms fluctuation levels of about 10%. The simple "strong turbulence" model thus has the effect of extending the range of validity of the theoretical results obtained using small perturbation theory, although for $\langle S_{PR}^2 \rangle$ the approximation is somewhat crude.

B. Theoretical Examples

The results summarized in Section III-A can be used to predict rms levels of fluctuations, $\langle B_{PR}^2 \rangle^{1/2}$ and $\langle S_{PR}^2 \rangle^{1/2}$, for a mobile parametric receiver. As the theoretical results depend strongly upon parameters of turbulence, some estimates for these parameters need to be made. It is shown in Ref. 10 that the pertinent parameters may be calculated as follows. The structure constant C_n is given by

$$C_n^2 \doteq 8.487 \times 10^{-8}\, v^2 L_o^{-2/3} \quad , \tag{5}$$

where

v is the velocity of the vessel in m/sec, and

L_o is the outer scale of turbulence, determined by dimensions of the flow around the pump transducer housing.

The mean square refractive index variations are

$$\langle \mu^2 \rangle \doteq 0.3162\ v/c_o \quad , \tag{6}$$

where c_o is the mean sound speed in m/sec. The mean correlation distance associated with the refractive index variations is given by

$$a = 6.699 \times 10^{-2} \sqrt{L_o} \quad . \tag{7}$$

Predictions of $\langle B_{PR}^2 \rangle^{1/2}$ and $\langle S_{PR}^2 \rangle^{1/2}$ can be made by substituting Eqs. (5)-(7) into Eqs. (1) and (2). Results of such predictions appear in Figs. 10, 11, and 12.

In Fig. 10, values of rms amplitude fluctuations $\langle B_{PR}^2 \rangle^{1/2}$ are shown as a function of array length L and pump frequency f_p. These values are calculated assuming v = 5 kt and L_o = 0.25 m (here L_o is approximated as the diameter of the wake behind the transducer). Note that, even at the low speed of 5 kt, significant levels of rms amplitude fluctuations are predicted for array lengths greater than 10 m and pump frequencies greater than 100 kHz. For example, with L = 20 m and f_p = 250 kHz, the predicted value of $\langle B_{PR}^2 \rangle^{1/2}$ is approximately 0.4. This means that the "output" of the parametric receiver (i.e., the sideband pressure detected by the hydrophone) will vary in amplitude by an rms amount of 40% of its mean value. As shown in the figure, this value of fluctuation increases with increasing pump frequency.

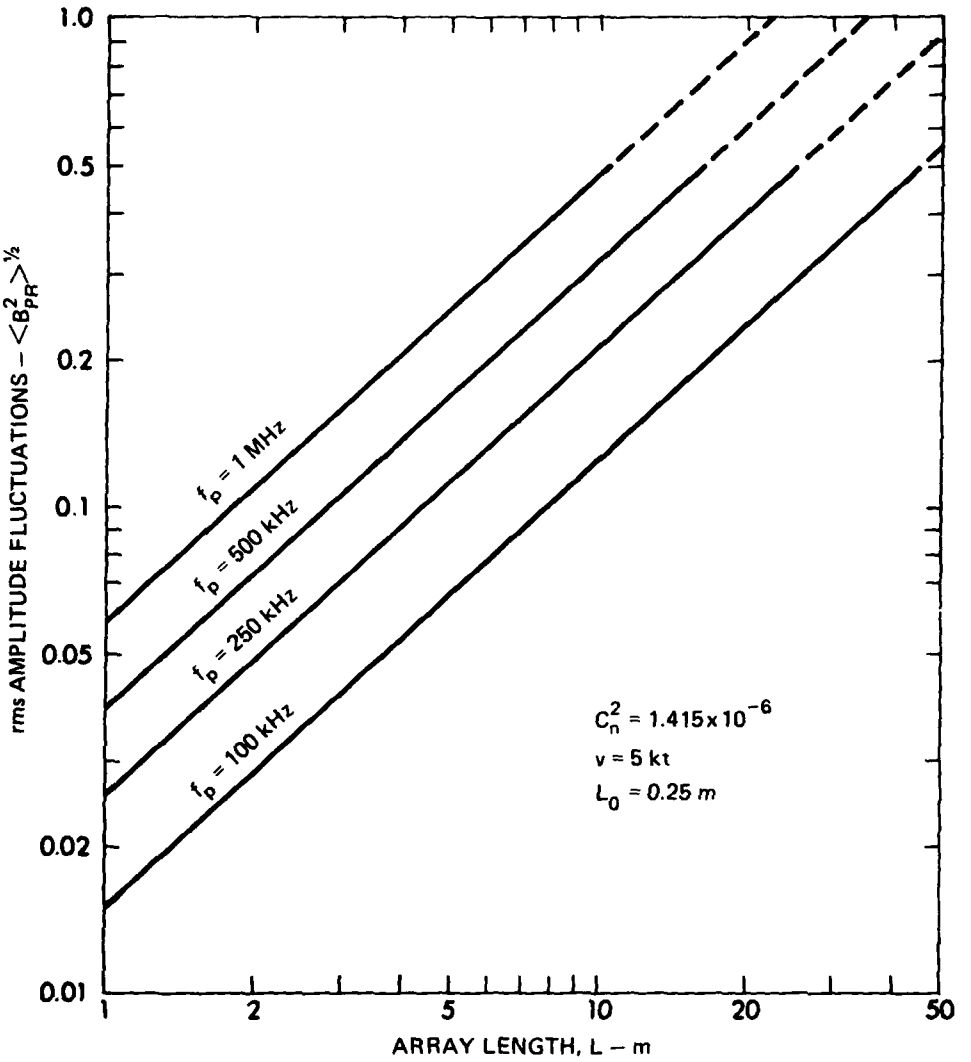

FIGURE 10
DEPENDENCE OF $\langle B_{PR}^2 \rangle^{1/2}$ UPON PUMP FREQUENCY

ARL:UT
AS-80-1781
RAL - GA
11 - 7 - 80

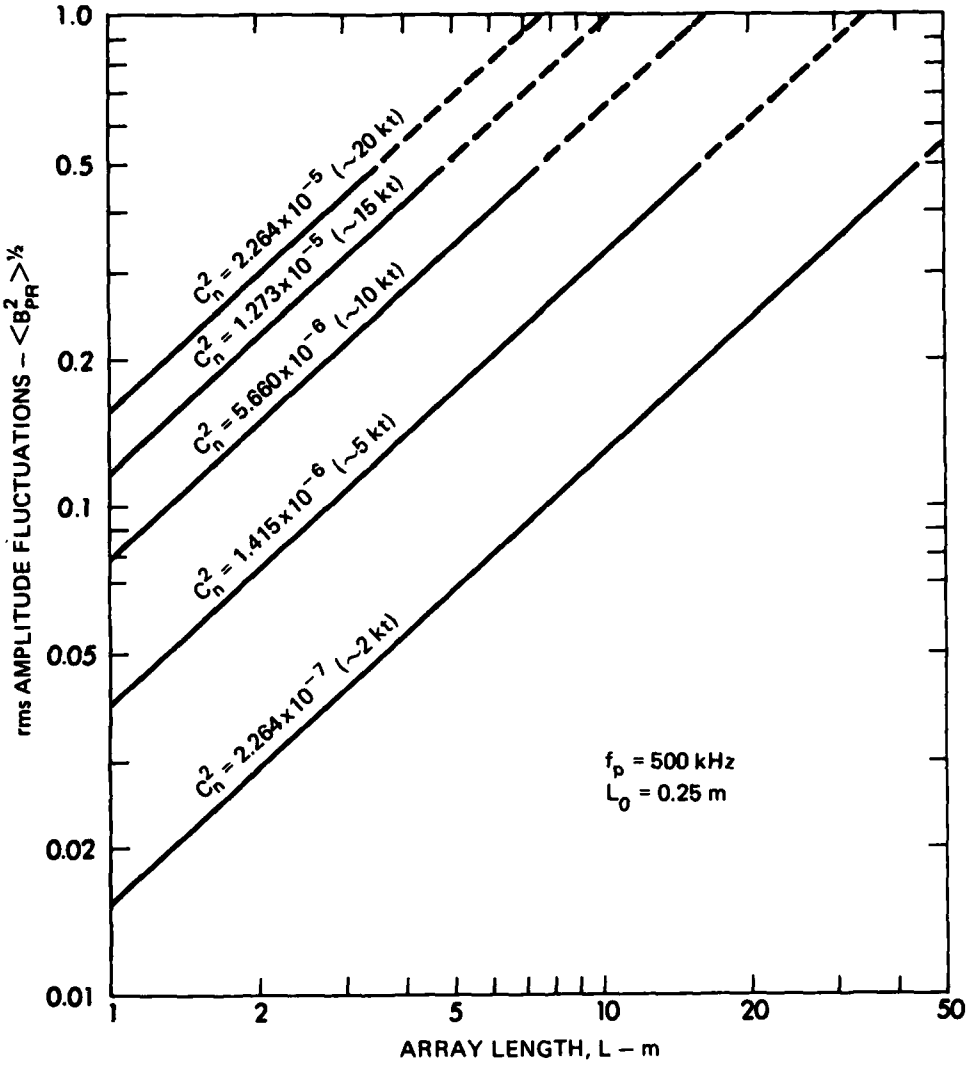

FIGURE 11
DEPENDENCE OF $\langle B_{PR}^2 \rangle^{1/2}$ UPON THE STRUCTURE CONSTANT

ARL:UT
AS-80-1782
RAL - GA
11 - 7 - 80

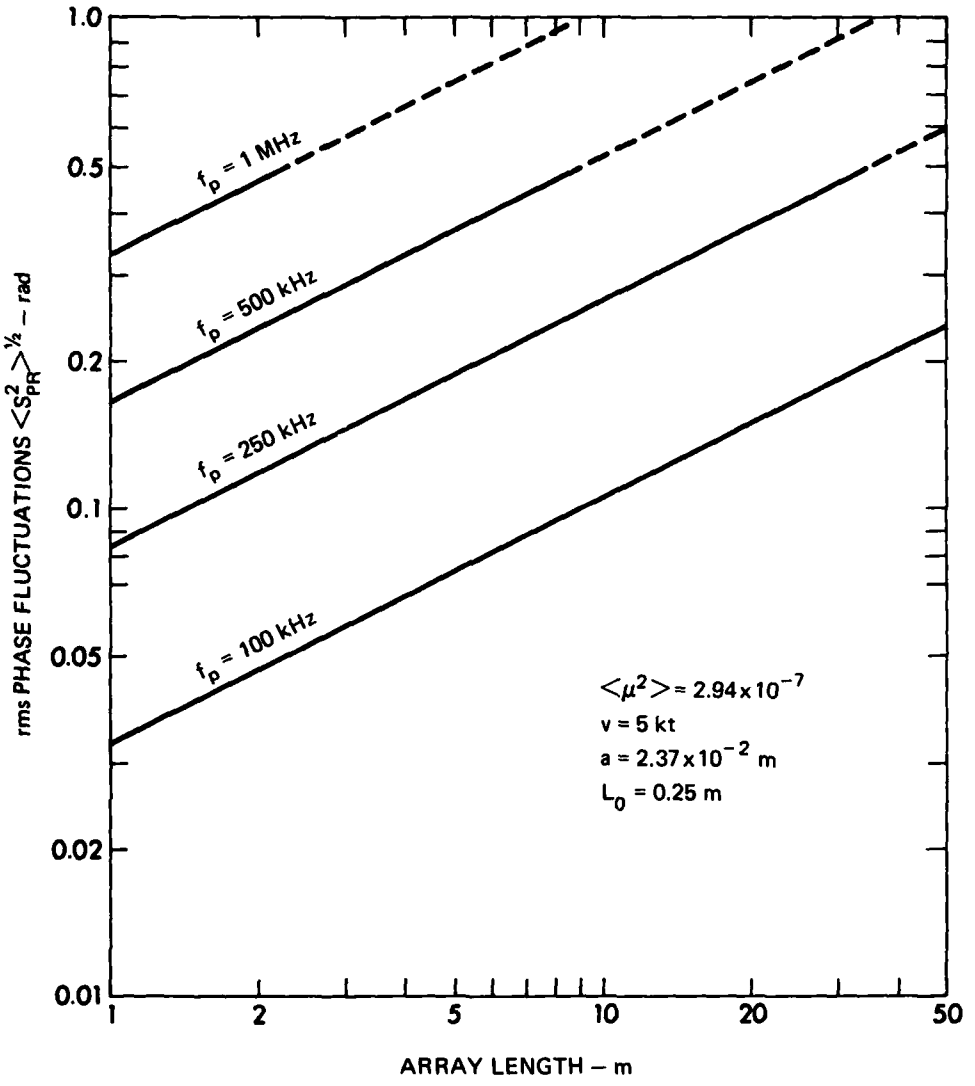

FIGURE 12
DEPENDENCE OF $\langle S_{PR}^2 \rangle^{1/2}$ UPON PUMP FREQUENCY

ARL:UT
AS-80-1783
RAL - GA
11 - 7 - 80

Similar results are shown in Fig. 11 for $\langle B_{PR}^2 \rangle^{1/2}$ as a function of array length L and structure constant C_n^2. Shown in parentheses are approximate values of boat speed to which the structure constants correspond. The pump frequency is assumed to be 500 kHz and L_o is again 0.25 m. Note that increasing boat speed produces a significant increase in the level of amplitude fluctuation for a given array length. For an array length of 20 m, the level of amplitude fluctuation exceeds the range of validity of the theory (i.e., $\langle B_{PR}^2 \rangle^{1/2}$ exceeds 0.5) for most values of C_n^2 shown.

Phase fluctuations as a function of array length and pump frequency are shown in Fig. 12. These values of rms phase fluctuations $\langle S_{PR}^2 \rangle^{1/2}$, in radians, are calculated for $\langle \mu^2 \rangle^{1/2} = 2.94 \times 10^{-7}$, which corresponds to a boat speed of approximately 5 kt and $L_o = 0.25$ m. The fluctuation levels in the figure are, for an array length of 20 m, generally in excess of 0.1 rad. Thus it can be seen from Fig. 12, that, for pump frequencies greater than 250 kHz and array lengths greater than 20 m, the phase fluctuations will have significant levels (in excess of 0.35 rad). The levels shown in Fig. 12 may be expected to increase with boat speed in a manner similar to that demonstrated by the amplitude fluctuations. For a pump frequency of 500 kHz, $\langle S_{PR}^2 \rangle^{1/2}$ will exceed 0.5 rad for speeds greater than 5 kt, even at short array lengths.

C. Conclusions and Future Work

The objective of the investigation, to analytically determine the effects of turbulence on mobile parametric reception, has been accomplished. Theoretical expressions have been developed for the amplitude and phase fluctuations produced by turbulence in the interaction region between pump transducer and hydrophone. Predictions have been made for the level of fluctuations that can be expected in practical applications. In this section, some conclusions are drawn from the results of the investigation, and future work is discussed.

The principal conclusion that can be made is that turbulence can produce significant variations in the amplitude and phase of an acoustic signal detected by the parametric receiver. For a 20 m long parametric receiver moving at a speed of 5 kt, it has been shown theoretically that rms amplitude variations exceed 50% of the mean amplitude, and rms phase variations exceed 0.5 radians, for pump frequencies of 500 kHz and higher.

A second conclusion that can be drawn from the theoretical results is that the level of the fluctuations is highly dependent upon the intensity and geometry of the turbulence present in the interaction region. Specifically, $\langle B_{PR}^2 \rangle$ is dependent upon the structure constant C_n^2 [see Eq. (3)] and $\langle S_{PR}^2 \rangle$ is dependent upon the mean square refractive index variations $\langle \mu^2 \rangle$ and the correlation distance, a.

This strong dependence of fluctuation levels upon the turbulence parameters means that the accuracy of any theoretical prediction of $\langle B_{PR}^2 \rangle$ or $\langle S_{PR}^2 \rangle$ is limited by the accuracy of the turbulence parameters used in making the calculation. These parameters are best determined experimentally, a point which leads to the third conclusion resulting from the investigation, that experiments are needed to determine the intensity and geometry of the turbulence that can be expected in a practical application. Some data regarding these turbulence parameters should permit predictions of the effects of turbulence on mobile parametric reception that would be more accurate than those presented in Section III-B.

Furthermore, experimental "testing" of the assumptions made in the theoretical analysis would extend the usefulness of the present study by defining the limits of its applicability. For example, it may be found that the assumptions of isotropic turbulence and of complete transverse correlation of fluctuations are valid only for certain velocities or for certain geometrical configurations.

Finally, there are two effects of turbulence that have not been considered in the present study. One is the spectral broadening of the

pump wave, which will contribute to the self-noise of the parametric receiver. This effect could reduce the minimum signal level that can be detected. A second effect is the noise generated by turbulence, both volume distributed noise and flow noise at the face of the hydrophone. This noise could also reduce the minimum detectable level of the parametric receiver. Both of these effects are more amenable to experimental than to theoretical study.

An experimental investigation generally dealing with the points discussed above has been proposed and will be sponsored by NAVSEA Code 63R, under Contract N00024-79-C-6358, Item 0034.

IV. SUMMARY

The parametric acoustic receiving array has characteristics that make it attractive as a possible passive sonar for mobile applications. It is capable of forming a conical receiving beam with minimum hardware in the water. However, the effects of both transducer vibration and turbulence offer possible constraints on the capability of a mobile PARRAY. These topics were investigated as reported in the previous sections.

It was found analytically and experimentally that the PLL receiver developed in this study is capable of greatly reducing the effects of transducer vibration on PARRAY performance. Typically, 30 dB attenuation of vibration induced sidebands was achieved using the PLL receiver.

It was determined analytically that turbulence can produce significant levels of amplitude and phase fluctuations in the signals detected by a mobile PARRAY. For a 20 m long PARRAY moving at 5 kt, it has been shown theoretically that rms amplitude fluctuations may exceed 50% of the mean amplitude, and rms phase fluctuations exceed 0.5 radians, for pump frequencies of 500 kHz and higher.

These fluctuations depend strongly upon the intensity and geometry of the turbulence present in the PARRAY interaction volume. Future experimental work is required to accurately determine the fluctuation levels that may be expected in practical applications.

REFERENCES

1. Tommy G. Goldsberry et al., "Development and Evaluation of an Experimental Parametric Acoustic Receiving Array (PARRAY)," Applied Research Technical Laboratories Report No. 79-5 (ARL-TR-79-5), Final Report under Contract N00039-76-C-0231, Applied Research Laboratories The University of Texas at Austin, 16 February 1979.

2. Tommy G. Goldsberry, Wiley S. Olsen, C. Richard Reeves, David F. Rohde, and M. Ward Widener, "PARRAY Technology Papers Presented at Scientific and Technical Meetings," Applied Research Laboratories Technical Report No. 79-4 (ARL-TR-79-4), Applied Research Laboratories, The University of Texas at Austin, 2 August 1979.

3. C. R. Reeves, T. G. Goldsberry, and D. F. Rohde, "Crossarray Beamforming With a Parametric Acoustic Receiving Array and a Broadside Line Array," IEEE Transactions on Aerospace and Electronic Systems AES-16, 180-190 (1980). (For revised version see Applied Research Laboratories Technical Paper ARL-TP-79-24, Rev., Applied Research Laboratories, The University of Texas at Austin, 16 June 1980.)

4. C. Richard Reeves, Tommy G. Goldsberry, David F. Rohde, and Voldi E. Maki, Jr., "Parametric Acoustic Receiving Array Response to Transducer Vibration," J. Acoust. Soc. Am. 67, 1496-1501 (1980).

5. F. M. Gardner, Phaselock Techniques, 2nd ed. (John Wiley & Sons, New York, 1979), pp. 8-9.

6. Donald L. Shilling and Marc Smirlock, "Intermodulation Distortion of a Phase Locked Loop Demodulator," IEEE Trans. Communication Technology COM-15, 222-228 (1967).

7. C. Melvil Thomas, "Distortion in the Phase-Locked Demodulator with Television and Multichannel Telephony," Proceedings National Electronics Conference XXIV, Chicago, Illinois, December 1968, pp. 396-401.

8. William C. Lindsey and Robert C. Tausworthe, "A Bibliography of the Theory and Application of the Phase-Lock Principle," JPL Technical Report 32-1581, Jet Propulsion Laboratory, Pasadena, California, 1 April 1973.

9. Robert A. Lamb, "Investigation of a Phase-Locked Loop Receiver for a Parametric Acoustic Receiving Array," Applied Research Laboratories Technical Report No. 80-25 (ARL-TR-80-25), Applied Research Laboratories, The University of Texas at Austin, 5 May 1980.

10. C. R. Culbertson, "Theoretical Analysis of the Effects of Turbulence on a Mobile Parametric Receiver," Applied Research Laboratories Technical Report No. 80-54 (ARL-TR-80-54), Applied Research Laboratories, The University of Texas at Austin, in preparation.

5 November 1980

DISTRIBUTION LIST FOR
ARL-TR-80-53
QUARTERLY PROGRESS REPORT NO. 4 AND FINAL REPORT
UNDER CONTRACT N00024-77-C-6200, ITEM 0011

Copy No.

Commander
Naval Sea Systems Command
Department of the Navy
Washington, DC 20362
1 Attn: Mr. C. D. Smith, Code 06R/63R
2 Dr. E. Liszka, Code 63R
3 Mr. D. E. Porter, Code 63R
4 CAPT R. H. Scales, PMS 402
5 Mr. D. L. Baird, Code 63X3
6 CDR D. F. Bolka, Code 63G
7 Mr. D. M. Early, Code 63D
8 Mr. John Neely, Code 63X3

Commander
Naval Electronic Systems Command
Department of the Navy
Washington, DC 20360
9 Attn: CAPT H. Cox, PME 124
10 Dr. J. A. Sinsky, Code 320A

Defense Advanced Research Projects Agency
1400 Wilson Boulevard
Arlington, VA 22209
11 Attn: CDR V. P. Simmons (TTO)
12 Dr. T. Kooij

Director
Naval Research Laboratory
Washington, DC 20375
13 Attn: Dr. M. Potosky, Code 5109
14 Dr. J. Jarzinski, Code 5131
15 Dr. R. D. Corsaro, Code 5131

Naval Research Laboratory
Underwater Sound Reference Division
P. O. Box 8337
Orlando, FL 32856
16 Attn: Dr. J. E. Blue
17 Dr. L. Van Buren
18 Dr. P. H. Rogers

Distribution List for ARL-TR-80-53, QPR No. 4 and Final Report Under Contract N00024-77-C-6200, Item 0011 (Cont'd)

Copy No.

Commanding Officer
Naval Ocean Systems Center
Department of the Navy
San Diego, CA 92152
19 Attn: Dr. H. Schenck, Code 71
20 Mr. M. Akers, Code 724
21 Dr. H. P. Bucker, Code 5311

Office of the Chief of Naval Operations
The Pentagon
Washington, DC 20350
22 Attn: CAPT R. G. Gilchrist, OP-95
23 Ms. J. C. Bertrand

Office of the Chief of Naval Operations
Long Range Planning Group
2000 North Beauregard Street
Alexandria, VA 22311
24 Attn: CAPT J. R. Seesholtz, Code 00X1

Officer-in-Charge
New London Laboratory
Naval Underwater Systems Center
Department of the Navy
New London, CT 06320
25 Attn: Dr. M. B. Moffett, Code 313
26 Mr. W. L. Konrad

Chief of Naval Research
Department of the Navy
Arlington, VA 22217
27 Attn: Mr. R. F. Obrochta, Code 464
28 Dr. L. E. Hargrove, Code 421

Commander
Naval Surface Weapons Center
White Oak Laboratory
Silver Spring, MD 20910
29 Attn: Dr. R. Coffman, Code U20

Commander
Naval Ocean Research and Development Activity
NSTL Station, MS 39529
30 Attn: Dr. A. L. Anderson, Code 320
31 Dr. S. W. Marshall, Code 340
32 Dr. J. Posey, Code 340

Distribution List for ARL-TR-80-53, QPR No. 4 and Final Report Under Contract N00024-77-C-6200, Item 0011 (Cont'd)

Copy No.

Commanding Officer
USCG Research and Development Center
Avery Point
Groton, CT 06340
33 Attn: CAPT M. Y. Suzich

34-35 Commanding Officer and Director
Defense Technical Information Center
Cameron Station, Building 5
5010 Duke Street
Alexandria, VA 22314

Battelle Memorial Institute
505 King Avenue
Columbus, OH 43201
36 Attn: TACTEC

Applied Research Laboratory
The University of Pennsylvania
P. O. Box 30
State College, PA 16801
37 Attn: Dr. F. H. Fenlon

Westinghouse Electric Corporation
P. O. Box 1488
Annapolis, MD 21404
38 Attn: Mr. A. Nelkin
39 Dr. P. J. Welton

Raytheon Company
Submarine Signal Division
P. O. Box 360
Portsmouth, RI 02871
40 Attn: Mr. J. F. Bartram

RAMCOR, Inc.
800 Follin Lane
Vienna, VA 22180
41 Attn: Mr. V. J. Lujetic

System Planning Corporation
1500 Wilson Blvd.
Arlington, VA 22209
42 Attn: Mr. J. Fagan

Distribution List for ARL-TR-80-53, QPR No. 4 and Final Report Under Contract N00024-77-C-6200, Item 0011 (Cont'd)

Copy No.

	Bolt, Beranek, & Newman, Inc. 50 Moulton Street Cambridge, MA 02138
43	Attn: Dr. J. E. Barger
44	Dr. F. J. Jackson
	Tracor, Inc. 6500 Tracor Lane Austin, TX 78721
45	Attn: Mr. D. F. Rohde
	Radian Corporation P. O. Box 9948 Austin, TX 78766
46	Attn: Dr. C. R. Reeves
	General Physics Corporation 10630 Little Patuxent Parkway Columbia, MD 21044
47	Attn: Dr. Frank Andrews
	Trans World Systems, Inc. 1311A Dolly Madison Blvd. McLean, VA 22101
48	Attn: Mr. Sam Francis
49	Office of Naval Research Resident Representative Room 582, Federal Building Austin, TX 78701
50	Physical Sciences Group, ARL:UT
51	Garland R. Barnard, ARL:UT
52	C. Robert Culbertson, ARL:UT
53	Tommy G. Goldsberry, ARL:UT
54	Robert A. Lamb, ARL:UT
55	T. G. Muir, ARL:UT
56	Reuben H. Wallace, ARL:UT
57	Library, ARL:UT
58-64	ARL:UT Reserve

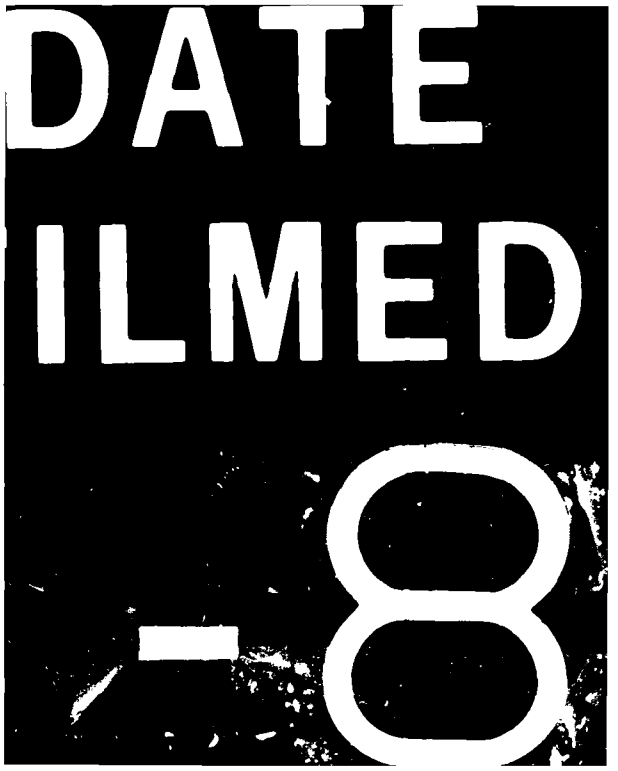
DATE
ILMED
-8